

Searching the Footprint of WIMPZILLAs

Houri Ziaeepour

*ESO, Schwarzchildstrasse 2, 85748, Garching b. München, Germany*¹

Email: houri@eso.org

Abstract

We constrain mass, lifetime and contribution of a very slowly decaying Ultra Heavy Dark Matter (UHDM) by simulating the cosmological evolution of its remnants. Most of interactions which participate in energy dissipation are included in the numerical solution of the Boltzmann equation. Cross-sections are calculated either analytically or by using PYTHIA Monte Carlo program. This paper describes in detail our simulation. To show the importance of the distribution of matter in constraining WIMPZILLA [1] characteristics, we consider two extreme cases: a homogeneous universe, and a local halo with uniform distribution. We show that in a homogeneous universe, the decay of UHDM with a mass $\sim 10^{15} GeV$ and a lifetime \sim a few times τ_0 the age of the Universe, can not explain the flux of observed Ultra High Energy Cosmic Rays (UHECRs). This shows the importance of nearby sources, notably galactic halo. In a uniform clump with an over-density of ~ 200 extended to $100 kpc$ or more, the lifetime must be $\sim 10 - 100 \tau_0$ or the contribution in the DM must be proportionally smaller. If the model developed by DIRBE group for estimating galactic IR underestimates the Galactic background or there is a significant galactic radio background, the lifetime can approach the lower limit of this range. We also compare our calculation with observed γ -rays at $E \sim 10^{11} eV$ by EGRET. It is compatible with uniform distribution of UHDM with relatively short lifetime.

1 First Encounter

Particle Physics today is a zoo with plenty of wild species very difficult to trace or capture. They are in general known under phyla WIMPs, LSP, Axions, Higgs, Heavy Neutrinos, etc. Most of these species are potential candidates of Dark Matter.

Recently a new phylum has been added to this zoo, WIMPZILLA [2]. The only common characteristic of the members of this family is their enormous mass, close to GUT scale $10^{16} GeV$ and their presumed long lifetime, much larger than the age of the Universe.

Theoretical motivations for existence of these particles is not very new. Since early 90s, some compactification scenarios in string theory predict composite particles (e.g *cryptons*) with large symmetry groups [3] and $M \sim 10^{14} GeV$ or greater. New class of string theories called M-theory [4] (heterotic strings and quantum gravity in 11-dim.) provides better candidates of large mass particles if the compactification scale is much larger than Standard Model weak interaction scale [5].

Another group and probably less fine-tuned candidates are messenger bosons. They provide the best way of soft supersymmetry breaking (see [6] for review). They communicate the SUSY breaking in the hidden sector to the observable (Standard Model) sector through loop correction of gauge fields. In most GUT-SUSY models, their mass must be close to GUT scale. They can have a long lifetime either if they are composite and decay only through non-renormalizable interactions or if they have a discrete gauge symmetry [7].

Production of ultra heavy particles could be restricted to very early Universe before GUT breaking and inflation if there was not a process to make them afterward. In this case, inflation diluted their density and they could not be part of Dark Matter today. However, parametric resonance [8] or vacuum fluctuation [2] at the end of inflation can produce a large amount of ultra heavy particles. The unitarity constraint on the mass of DM particles [9] can be turned over if they have never been thermalized [2]. If there was not other motivation for existence of an ultra heavy meta-stable particle, it was just one of many predictions of Particle Physics models waiting detection. However, probably we have already

¹Present Address: 03, impasse de la Grande Boucherie, F-67000, Strasbourg, France.

some *observed* indication of their existence: Ultra High Energy Cosmic Rays (UHECRs) detected by large Air Shower detectors [10] [11] [12] (For a review of UHECRs detection and observed properties see [13]). The GZK cutoff [14] in the spectrum of CRs at energies around $\sim 10^{18}eV$ (the exact place of the cutoff depends on the amount and distribution of sources and IR background) due to interaction with CMBR and IR photons restricts the distance to sources of these particles to less than $20 - 30 Mpc$. At present there are about 600 events with $E \sim 10^{19}eV$, 50 with $E > 4 \times 10^{19}eV$ and 14 events with $E > 10^{20}eV$ [15] [16] including one with $E \sim 10^{21}eV$ [11]. The UHECR spectrum has a local minimum around $E \sim 10^{19}eV$ but it rises again at higher energies.

It is possible to estimate the composition of the primary particle [17] [18] from determination of the shower maximum position and its elongation rate in the atmosphere as well as the same parameters for muon content of the shower. However, uncertainties in observations and detector models don't permit to determine the nature of the primary with a great accuracy. Moreover, conclusions depend on the interaction model of hadrons at high energies [19]. In spite of these uncertainties, all observations and analysis of the data from different detectors and by different groups are compatible with a composition change from iron nuclei to proton at energies $> 10^{18}eV$ [11] [17] [18]. Nevertheless, based on theoretical arguments, some authors suggest that the highest energy events can be produced by heavy nuclei [20] (But see also [21] for maximum fly distance of *Fe* nuclei).

1.1 Sources

During few years since the first observation of UHECRs and specially after the detection of the most energetic event ever observed by Fly's Eye [11], numerous works have been performed to understand the origin and propagation of these particles. A review of part of these ideas can be found in [22] and references therein. For the sake of completeness here we briefly review arguments for and against conventional and exotic sources.

1.1.1 Classical Candidates

In a recent review of conventional candidates [23] of UHECRs, R. Blandford rules out practically all of them.

The most promising non-exotic candidate for the UHECR sources is the acceleration of charged particles in the shock waves of AGNs, SNs, or in-falling gas in rich clusters. The main condition for these objects to be able to produce the observed spectrum of UHECRs is the existence of a coherent and enough strong magnetic field at large scale, pc/kpc for AGNs and SNs, Mpc for clusters.

The maximum acceleration energy that a charged particle can achieve is $E_{max} = e\mathcal{E} \sim euB\mathcal{R}$, where e is charge, \mathcal{E} electric field, u speed, B magnetic field, and \mathcal{R} the size of the accelerator. For direct ejection of charged particles from source $\mathcal{R} > r_L = \frac{E}{eB}$, r_L is the Larmor radius of the particle.

Using this simple estimation, remnants of old SNs are expected to accelerate protons up to $\sim 10^{15}eV$ and iron to $\sim 10^{18}eV$ [24]. A $\sim 100TeV$ γ -ray is expected from synchrotron radiation of these protons. However, for the time being, all attempts have failed to detect them [25].

Shock front of AGNs relativistic jets with $\mathcal{R} \sim 0.1pc$ and $B \sim 30G$ [26] can accelerate protons to or close to $\sim 10^{21}eV$. Central black hole in Fannaroff-Riley galaxies [27] with $\mathcal{R} \sim 10^{-3}pc$ and $B \sim 5G$ or the remnant of QSO [28] can produce UHECRs up to energies $\sim 10^{20}eV$ with a marginal maximum energy of $4 \times 10^{21}eV$ [29].

Estimation of maximum acceleration energy does not take into account energy loss in the adiabatic expansion [30] which can be orders of magnitude, as well as *in situ* interaction with radiation and matter fields which are extremely strong in the objects that can accelerate protons to such extreme energies. One way out of adiabatic energy loss is an abrupt termination of the acceleration zone. This needs a fine-tuning in the structure of the source but is not ruled out. Another possibility is composition change from p to n [30] by interaction with photons. We show below that hadronic jet production in this process

reduces the mean energy of the nucleon significantly. Consequently, outgoing particles should have a mean energy much less than theoretical maximum energy.

The production flux of UHECRs is another issue. As it is not very well understood even at low energies, usually an extrapolation of spectrum from low energies is assumed.

Gamma Ray Bursts (GRB) also have been proposed as the candidate source for UHECRs [31]. The main argument for this suggestion is the observation of TeV background excess in the direction of GRBs. They can be due to synchrotron radiation of protons with $\sim 10^{20} eV$. A simulation [32] of cosmological distribution of sources with a power law flux of UHECRs shows that the expected flux on Earth is much lower than observed value. However, authors argue that the statistical expectation of 1.3 events with $\sim 10^{20} eV$ is compatible with observation. Today, after detection of at least 14 events in this energy range, the simulation certainly does not reproduce observations. Waxman & Coppi [32] predict also an excess of $> 1TeV$ secondary photons due to interaction with CMBR and IR photons, in the direction of UHECRs with a delay of $\sim 10^3 hr$ that has not been observed either.

In a recent simulation of propagation of UHECRs from a bursting source [33], it has been argued that Poisson noise in the process of proton interaction with background photons leaves a non-interacting tail in the flux of UHECRs that increases the probability of detecting UHECRs from further distances. For high energy protons the interaction rate with CMBR is $\sim 0.2 Mpc^{-1}$. This means that the probability of non-interacting in a distance of $30 Mpc$ is only 0.25%. Moreover, the effect of Poisson noise has to be observed in the spectrum of a source. It should produce abrupt features due to 1 interaction, 2 interactions, etc.

1.2 Correlation with Astronomical Objects

In searching for a candidate astronomical source, one has to consider a number of issues: If UHECRs are protons, the source must be in a distance permitted by GZK cutoff. For energies $< 10^{19} eV$, the deviation of charged particles by galactic and super-galactic plane magnetic fields can be important [34] [35] [36] [37] [33]. Moreover, for pointing to a source, one has to take into account the poor angular resolution of detectors ($\sim 2^\circ$).

At present no serious candidate source has been observed. A correlation between Super Galactic Plane and UHECR events direction has been claimed [38], but ruled out by other analyses [39]. Another claim of clustering comes from AGASA collaboration [15]. They find that 7 most energetic events ever observed can be divided to two doublets and one triplet. Regarding the small statistics of the data, this claim is very speculative. For instance, there is 3 years of time separation between two members of one of the doublets. In addition, it is very plausible that apparent correlation come from caustics generated by galactic magnetic field [34] [40].

Most of UHECRs burst models predict only one important nearby source of UHECRs [31] [33]. M87 in Virgo Cluster is practically the only conventional candidate that respects the distance constraint of GZK cutoff and is probably able to accelerate protons to ultra high energies. Recently it has been shown that galactic wind and its induced magnetic field can deflect protons with $E > 10^{20} eV$. If the magnetic field is as high as $7 \mu G$ (which is somehow higher than what observations suggest), most of these events point to Virgo Cluster [40]. However, even with this strong magnetic field, Galactic wind model studied in [40] can correlate the highest energy events with M87/Virgo only if the primaries are He nuclei.

There are also claims of correlation between the direction of UHECRs and pulsars [41] or QSOs [42]. The latter is reliable only if UHECRs are neutrinos. This is in contradiction with observed composition of UHECRs. If ultra high energy neutrinos interact with a halo of massive neutrinos around Milky way and produce protons, QSOs can be considered as potential sources [43]. But the present limits of few eV on the neutrinos mass reduces the probability of existence of a neutrino halo. Even in presence of a halo, the effect of background neutrino seems to be more important and neutrinos lose their energy in cosmological distances [44].

If UHECRs originate from some type of Dark Matter, e.g. UHDM, black holes in the Galactic Halo or

decay of topological defects, their distribution must show an anisotropy of 10% to 40% depending on the halo model [45] [46]. N. Hayashida *et al.* [47] reports a small excess of $\sim 4\%$ for UHECRs with energies $\sim 10^{18} eV$ in the direction of the Galactic Center and Cygnus region. Based on this argument and using all the present data from different detectors, Benson, *et al.* [48] rule out the DM origin of UHECRs. However, a more complete study including a model for galactic magnetic field [49] concludes that the statistics of the present data is too low to be conclusive. It only puts a lower limit on the flatness of the Halo $q > 0.4$.

In what concerns the anisotropy of UHECRs, a crucial contributor is the bias between baryonic and non-baryonic DM. The observed density and distribution of MACHOs is compatible with an inner halo (at least up to 50 kpc) that a significant fraction of its mass is composed of these presumably baryonic objects. Contribution of MACHOs becomes more important for a flatter halo. This baryonic inner halo influences arguments for and against an UHDM in various ways. On the one hand it reduces the expected anisotropy as well as flux of UHECRs from non-baryonic DM on Earth. In fact if we extrapolate the anisotropy calculated by S. Dubovsky & P. Tinyakov [45] (their Fig.1) to a core radius of 50 kpc, it approaches to 1, i.e. no anisotropy. On the other hand, observations show that a larger contribution of MACHOs in the halo mass needs a flatter halo and thus more anisotropy in the UHECRs direction if they come from a DM halo. Present data is not conclusive specially because we don't have reliable data from southern hemisphere. Auger detector will improve our knowledge about distribution of UHECRs. In conclusion, our present knowledge and modeling of numerous phenomena which influence production and propagation of UHECRs is incomplete. A realistic model must include a better model of halo and its compositions, Galactic backgrounds, all component of magnetic field including wind, and energy dissipation of UHECRs by interaction with radio, CMB & IR photons and with matter. This latter issue will be partly discussed in this work. A better understanding of CR production by conventional sources also is crucial.

1.3 Exotic Sources

Another possible class of sources is the decay of a very heavy elementary particle with a GUT-scale mass [50]. These particles can be either long life very heavy particles, or short life particles produced by decay of topological defects. In the latter case, the heavy particles decay in their turn to ordinary particles and make the observed UHECRs.

The possibility that topological defects be the source of UHECRs has been studied extensively ([51], [22] and references therein). Topological defects are relics from the early universe, produced during various stages of phase transition [52]. Due to spontaneous symmetry breaking, part of space gets a topologically non-trivial configuration of the order-parameter (field) different from the rest of the universe. This state can not decay by its own, but processes like cosmic strings 'collision', collapse of macroscopic loops, loop shrinking, monopole-anti-monopole annihilation, etc. can distort the field configuration and destroy it. In this situation, the energy from the order parameter will be transferred to gauge bosons and/or the oscillation of the field produces Higgs with a mass of the same scale as the phase transition scale. These heavy particles subsequently decay to light particles that contribute to UHECRs.

The result of the decay of a heavy short life particle and a heavy relic can be quite the same, but their production rate and its evolution with time is very different and specially in the case of topological defects it depends on the defect type and model [51].

Some years ago, there was a lot of hopes and attempts to prove that topological defects can be the seed of LSS and CMB fluctuations. However, the results of comparison between simulations and observed power spectrum of LSS and CMB anisotropy practically rules out this possibility [53]. Even recent attempts to combine inflation and local strings show that the contribution of topological defects in the early universe can not be more than 20% [54].

Another proposed source of UHECRs is the evaporation of primordial black holes. At the end of their life, the Hawking temperature of these objects is enough high to produce extremely energetic elementary

particles like quarks and gluons. Their hadronization can produce the observed UHECRs. Most of models for production of PBH needs fine tuning to not produce too much of them. Moreover, PBH with present temperature of same order as UHECRs energy must have an initial mass of $10^{14} - 10^{15} gr$. They are mainly produced when a large over density region crosses the horizon [55]. Assuming a radiation dominated universe, this range of horizon mass happens when the temperature of the universe is $\sim 10^9 GeV$. This energy scale is larger than the scale of thermal inflation and PBH density would be reduced $\sim 10^{12}$ times after if a thermal inflation [56] happens at EW scale. In models with low reheating temperature, at these scales the Universe is not yet thermalized and parametric resonance and fluctuation production happens only for superhorizon scales [8]. Therefore, it seems that horizon scale over-densities must be too rare to produce PBH with necessary mass in enough amount.

Summarizing the discussion of this section, it seems that conventional sources of Cosmic Rays are not able to explain the observed rate of UHECRs [23]. Between exotic sources, the decay of a meta-stable ultra heavy particle seems to be the most plausible source.

The decay of UHDM can have important implications for the evolution of high energy backgrounds. This can also be used for verification of this hypothesis and constraining the mass and lifetime of these particles. A number of authors have already tried to estimate possible range of these parameters as well as the flux of remnants on Earth ([57] and [58] for defects, [59], [60] and [61] for UHDM). The essential difference of present work with others is that more interactions have been included in analyzing the energy dissipation of UHDM remnants. In addition, non-perturbative interactions and hadronization are added by using results of PYTHIA Monte Carlo program [62]. We try to find the range of mass and lifetime of UHDM that can explain observed flux of UHECRs and high energy Gamma-Ray background observed by satellites and ground based detectors. We consider two distributions for UHDM. First we study the evolution of the spectrum of stable particles i.e. $e^\pm, p^\pm, \nu, \bar{\nu}$ and γ in a homogeneous universe from photon decoupling to today. Then to show the effect of matter clumpiness, we simulate the Galactic Halo by simply considering a uniform over-density. A complete treatment of a clumpy universe will be reported elsewhere. We also try to estimate the effect of very slow decay of DM in the equation of state of the Universe and in baryon and lepton asymmetries.

2 WIMPZILLA Decay and Energy Dissipation of Remnants

In this section we describe the decay model of UHDM and interactions which are included in the simulation.

2.1 Decay Model

Theoretical predictions for mass and lifetime of UH particles cover a large range of values $m_{UH} = 10^{22} - 10^{26} eV$ and $\tau_{UH} = 10^7 - 10^{20} yr$ [3] [5] [63]. Nevertheless, at the end of inflation it is more difficult to produce the highest range of the masses and special types of inflationary models [64] are needed. For UH particles make a substantial part of the Dark Matter today, their lifetime must be at least comparable to the age of the Universe. In this work we perform the simulation for $m_{UH} = 10^{22} eV$ and $m_{UH} = 10^{24} eV$. They are reasonable values if we want $m_{UH} \lesssim$ GUT scale $= 10^{16} GeV$. For lifetime, $\tau_{UH} = 5\tau_0$ and $\tau_{UH} = 50\tau_0$, where τ_0 is the age of the Universe are studied. These values are smaller than what have been used by other groups [59] [61]. We show below that taking into account a realistic model for energy dissipation of remnants, even these relatively short lifetime **can not** explain the flux of UHECRs in a homogeneous universe. For some halo and IR background models, these lifetimes or slightly larger ones are compatible with observations.

The decay modes of UHDM are very model dependent. It is very likely that they don't decay directly to known particles and their decay has a number of intermediate unstable states that decay in their turn. It is also very probable that remnants includes stable WIMPs which are not easily observable. To study

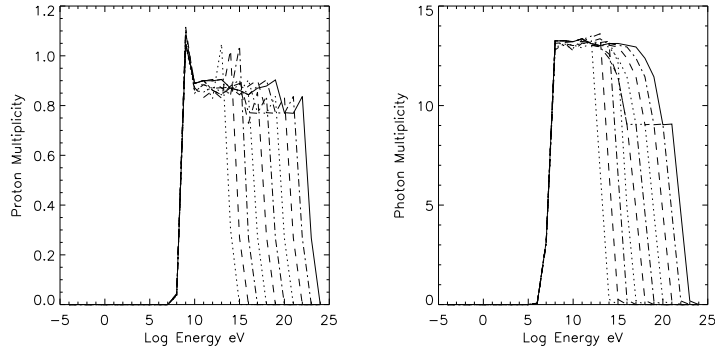


Figure 1: Proton and photon multiplicity in hadronization of a pair of gluon jets for $E_{CM} = 10^{14} - 10^{24} eV$.

the maximal observable effects of the decay on high energy backgrounds, we assume that at end, the whole decayed energy goes to stable *visible* particles.

In most WIMPZILLA models, these particles are neutral bosons. Due to lack of precise information about their decay, we assume that it looks like the decay of Z^0 . Theoretical and experimental arguments show that leptonic and hadronic decay channels of Z^0 have a branching ratio of $\sim 1/3 - 2/3$ [65]. As the dominant channel is the hadronic one, here we only consider this mode. It maximizes the flux of nucleons which at present are the dominant observable at ultra high energies.

To mimic the softening of energy spectrum due to multiple decay level, we assume that decay is similar to hadronization of a pair of gluon jets. Experimental observation [66] as well as MLLA (Modified Leading Logarithm Approximation) [67], LPHD (Local Parton-Hadron Duality) ([68] and references therein) and string hadronization model [69] obtain a softer spectrum with higher multiplicity for gluon jets than for quarks.

We use PYTHIA program [62] for jet hadronization. This program, like many other available ones, can not properly simulate ultra high energy events, not only because we don't know the exact physics at $10^{16} GeV$ scale, but also because of programming limits. For this reason, we had to extrapolate simulation results from lower energies. Fig.1 shows as an example, proton and photon multiplicity in hadronization of a pair of gluon jets. At middle energies, the multiplicity per $\log(E)$ is roughly constant. The same behavior exists for other species. This is a known shortcoming of present fragmentation simulations [70] (See also Appendix 1) and makes spectrum harder at middle energies. As we would like to study the maximal flux of UHECRs and their effects on high energy backgrounds, this problem can not change our conclusions.

In the simulation, all particles except $e^\pm, p^\pm, \nu, \bar{\nu} \& \gamma$ decay. We neglect the mass of neutrinos and for simplicity we assume only one family of neutrinos i.e. ν_e .

Contribution of stable species in total multiplicity and total decay energy is summarized in Table 1. It shows that mass of UHDM has little effect on the composition of remnants. For all species, more than 99% of the total energy belongs to the particles with energies higher than $10^{20} eV$ and $10^{18} eV$ respectively for two masses.

2.2 Interactions

We included roughly all relevant interactions between remnants (except $\nu - \nu \& \bar{\nu} - \bar{\nu}$ elastic scattering) to the simulation either analytically or by using the results of PYTHIA Monte Carlo. Previous works [57] [58] [59] [61] either don't consider the energy dissipation or take into account only first order perturbative interactions (except $p - \gamma$ where a fitting is used for $N - \gamma \rightarrow N - \pi$ cross-section). An early version of the simulation presented here [60] studied only energy dissipation of UHECRs using PYTHIA

Table 1: Energy and multiplicity contribution in remnants of WIMPZILLA

Part.	$M_{DM} = 10^{24} \text{ eV}$		$M_{DM} = 10^{22} \text{ eV}$	
	Ener. %	Multi. %	Ener. %	Multi. %
e^\pm	6.7	9.7	6.7	9.8
p^\pm	11.8	1.4	11.9	1.4
$\nu & \bar{\nu}$	18.4	28.3	18.1	28.3
γ	26.2	21	26.6	21

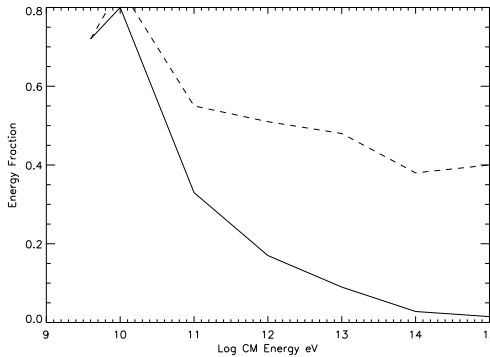


Figure 2: Energy fraction of leading proton (dashed line) and mean energy of protons (solid line) with respect to the incoming proton energy in $p - \gamma$ interaction.

without considering interactions of secondary particles. It didn't include low energy processes and found a higher lifetime for UHECRs than present work.

The main reason for considering only first order interactions is that it is usually assumed that CMB photons are the main source of energy dissipation of UHECRs. This argument is true. However, in the galactic medium, the IR and visible radiations are comparable with CMB and play an important role in the energy dissipation of protons of $E \sim 10^{19} - 10^{20} \text{ eV}$. In extragalactic medium, the number density of background high energy photons with ($E > 1 \text{ eV}$) is larger than visible and near IR. Another factor which accelerates energy dissipation of protons in interaction with high energy photons is energy loss of leading proton in $p - \gamma$ interaction. It increases with energy (See Fig.2) and results a higher dissipation rate. In conclusion, it seems necessary to take into account non-perturbative interactions.

PYTHIA can not simulate interactions with invariant CM energies $E_{CM} \equiv \sqrt{s}$, $E_{CM} < 2 \text{ GeV}$ to $E_{CM} < 4 \text{ GeV}$ (the lower limit depends on the interaction). Consequently, for smaller energies we have included only perturbative, first order interactions using analytical expressions. Table 3 summarizes all the interactions which are included in the simulation, the energy range of analytical and/or Monte Carlo calculation of the cross-sections, and the cuts used for removing infinities at small energies or angles in the case of analytical calculation (results depend somehow on these cuts specially in the case of moderate energy and angular resolution of our program). For energy ranges that PYTHIA has been used, in general we use default value of various parameters of the program as defined in PYTHIA manual. A number of parameters are changed for all processes e.g. to make unstable particles like mesons decay etc. They are listed in Table 2. For some interactions, the value of a few other parameters are changed. They are also listed in the Table 3. From now on s , t and u are Mandelstam variables.

At very high energies, $E_{CM} > 10^{14} \text{ eV}$ for nucleon-nucleon and $E_{CM} > 10^{15} \text{ eV}$ for other interactions, PYTHIA becomes very slow and the number of rejected events increases rapidly. For these energies we

Table 2: PYTHIA Parameters

Selected processes	lept.-lept, lept.-had., unresolved γ , low p_t , diffract. & elastic had.-had., Radiative correction
Status parameters	2^{ed} -order α_s , continuous p_t cutoff.
Pt cuts	$E_{CM}^{min} = 1$, $p_t^{min} = 0$
Number of flavors	6

perform a linear extrapolation from lower energies as explained below.

3 Evolution

We assume that non-baryonic Dark Matter is totally composed of slowly decaying UH particles. From now on, any reference to DM means this type of dark matter. Boltzmann equation for space-time and energy-momentum distribution of a particle i is [73](We use units with $c = \hbar = 1$):

$$p^\mu \partial_\mu f^{(i)}(x, p) - (\Gamma_{\nu\rho}^\mu p^\nu p^\rho - e_i F_\nu^\mu p^\nu) \frac{\partial f^{(i)}}{\partial p^\mu} = -(\mathcal{A}(x, p) + \mathcal{B}(x, p)) f^{(i)}(x, p) + \mathcal{C}(x, p) + \mathcal{D}(x, p) + \mathcal{E}(x, p). \quad (1)$$

$$\mathcal{A}(x, p) = \Gamma_i m_i. \quad (2)$$

$$\mathcal{B}(x, p) = \sum_j \frac{1}{(2\pi)^3} \int d\bar{p}_j f^{(j)}(x, p_j) A(s) \sigma_{ij}(s). \quad (3)$$

$$\mathcal{C}(x, p) = \sum_j \Gamma_j m_j \frac{1}{(2\pi)^3} \int d\bar{p}_j f^{(j)}(x, p) \frac{d\mathcal{M}^{(i)}}{d\bar{p}}. \quad (4)$$

$$\mathcal{D}(x, p) = \sum_{j,k} \frac{1}{(2\pi)^6} \int d\bar{p}_j d\bar{p}_k f^{(j)}(x, p_j) f^{(k)}(x, p_k) A(s) \frac{d\sigma_{j+k \rightarrow i+\dots}}{d\bar{p}}. \quad (5)$$

$$d\bar{p} = \frac{d^3 p}{E} \quad (6)$$

x and p are coordinate and momentum 4-vectors; $f^{(i)}(x, p)$ is the distribution of species i ; m_i , e_i and Γ_i , are its mass, electric charge and width $= 1/\tau_i$, τ_i is the lifetime; σ_{ij} is the total interaction of species i and species j at a fixed s ; $\frac{d\sigma_{j+k \rightarrow i+\dots}}{d\bar{p}} = \frac{E d\sigma}{\bar{p}^2 d\bar{p} d\Omega}$ is the Lorantz invariant differential cross-section of production of i in the interaction of j and k . Here we treat interactions classically, i.e. we consider only two-body interactions and we neglect the interference between outgoing particles. It is a good approximation when the plasma is not degenerate. It is assumed that cross-sections include summation over internal degrees of freedom like spin; $\frac{d\mathcal{M}^{(i)}}{d\bar{p}}$ is the differential multiplicity of production of species i in the decay; $\Gamma_{\nu\rho}^\mu$ is the connection and F_ν^μ an external electromagnetic field. $A(s)$ is the kinematic factor [74] and depends on the invariant square mass of the initial particles $s = m_i^2 + m_j^2 + 2p_i \cdot p_j$:

$$A(p_i, p_j) = ((p_i \cdot p_j)^2 - m_i^2 m_j^2)^{\frac{1}{2}} = \frac{1}{2} ((s - m_i^2 - m_j^2)^2 - 4m_i^2 m_j^2)^{\frac{1}{2}}. \quad (7)$$

The quantity $A\sigma$ presents the probability of an interaction. Equation (1) must be coupled to Einstein equation:

$$R_{\mu\nu} - \frac{1}{2} g_{\mu\nu} R = 8\pi G T_{\mu\nu} + \Lambda g_{\mu\nu}. \quad (8)$$

Equations (1) and (8) are connected through definition of $T_{\mu\nu}$:

$$T_{\mu\nu} = \frac{g}{(2\pi)^3} \int p_\mu p_\nu f(x, p) d\bar{p}. \quad (9)$$

The term $\mathcal{E}(x, p)$ in (1) presents interaction with external sources.

3.1 Homogeneous Universe

In a homogeneous universe $f(x, p) = f(t, |p|)$ and in (1) the term corresponding to interaction with external electromagnetic field is zero. Therefore, to have a consistent formalism for evolution of distribution of all species, we don't include the synchrotron radiation of high energy electrons in a magnetic field. We only consider the evolution of stable particles listed in previous section and slowly decaying UHDM. The term (2) concerns only UHDM. In (4), the only non-zero term in the sum is the decay of UHDM. We assume that stable species don't have any interaction with UHDM and corresponding interaction integrals in (3) and (5) are zero.

For simplicity we assume that the non-baryonic dark matter is composed only of UHDM. From (2) and (4) it is evident that width and fraction of UHDM in DM are degenerate and in evolution equations, decreasing contribution is equivalent to increasing lifetime. For numerical calculations, it is simpler to assume that DM is only composed of UHDM and adjust the lifetime.

Due to very large mass of UHDM, its momentum is negligible and we can assume that in comoving frame it is at rest. This permits to use its number density n_{DM} which is more convenient for numerical calculation.

In a homogeneous universe the metric in comoving frame is:

$$ds^2 = dt^2 - a^2(t) \delta_{ij} dx^i dx^j. \quad (10)$$

and with respect to local Lorentz frame (1) to (5) take the following form (in the following the species index indicates one of the stable species):

$$\frac{\partial f^{(i)}(t, p)}{\partial t} - \frac{\dot{a}}{a} p \frac{\partial f^{(i)}}{\partial p} = \frac{1}{E} (-\mathcal{B}(t, p) f^{(i)}(t, p) + \mathcal{C}(t, p) + \mathcal{D}(t, p)). \quad (11)$$

$$\mathcal{B}(t, p) = \sum_j \frac{1}{(2\pi)^3} \int dp_j \frac{p_j^2}{E_j} f^{(j)}(t, p_j) \int d(\cos \theta_{ij}) A(s) \sigma_{ij}(s). \quad (12)$$

$$\mathcal{C}(t, p) = \frac{E}{4\pi g_i p^2} \Gamma_{DM} n_{DM} \frac{d\mathcal{M}^{(i)}}{dp}. \quad (13)$$

$$\mathcal{D}(t, p) = \sum_{j, k} \frac{1}{(2\pi)^6} \int dp_j dp_k \frac{p_j^2}{E_j} \frac{p_k^2}{E_k} f^{(j)}(t, p_j) f^{(k)}(t, p_k) \int d(\cos \theta_{jk}) d(\cos \theta_{ji}) d\phi_i A(s) \frac{d\sigma_{j+k \rightarrow i+...}}{d\bar{p}}. \quad (14)$$

$$\frac{dn_{DM}}{dt} + \frac{3\dot{a}}{a} n_{DM} = -\Gamma_{DM} n_{DM}. \quad (15)$$

In (12) and (14) s depends on the angle between species j and k , and j and i . Consequently, it is not possible to use cross-sections integrated on angular variables.

Evolution of $a(t)$ is ruled by Einstein equation:

$$\frac{\dot{a}^2}{a^2} = \frac{8\pi G}{3} T_{00} + \frac{\Lambda}{3}. \quad (16)$$

$$T^{00}(t) = \sum_i \frac{g_i}{2\pi^2} \int dp p^2 E f^{(i)}(t, p). \quad (17)$$

g is the number of internal degree of freedom (e.g. spin, color) of particles. Equations (11) and (16) determine the cosmological evolution of species. Due to interaction terms, even in a homogeneous universe, these equations are non-linear and coupled. It is not therefore possible to solve them analytically.

Evolution equation for DM can be solved analytically. For other species if in (11) we consider absorption and production integrals as t and p dependent coefficients of a linear partial differential equation, (11) can be solved analytically [75]. Giving the value of $f^{(i)}(t, p)$, $n_{DM}(t)$ and $a(t)$, at time t , we can then determine $a(t + \Delta t)$, $n_{DM}(t + \Delta t)$, $\mathcal{B}(t, p)$, $\mathcal{C}(t, p)$ and $\mathcal{D}(t, p)$ for a short time interval Δt . $f^{(i)}(t + \Delta t, p)$ would be obtain from solution of partial differential equation (11) using difference method. This prescription is more precise than a pure numerical calculation e.g. difference method.

The solution of metric and distributions in one step of numerical calculation are the followings:

$$a(t + \Delta t) = a(t) \exp(\Delta t(8\pi G 3T_{00} + \frac{\Lambda}{3})^{\frac{1}{2}}). \quad (18)$$

$$n_{DM}(t + \Delta t) = n_{DM}(t) \frac{a^3(t_0)}{a^3(t)} \exp(-\frac{t - t_0}{\tau}). \quad (19)$$

$$f^{(i)}(t + \Delta t, p) = (f^{(i)}(t, p') + \Delta t(\mathcal{C}(t, p') + \mathcal{D}(t, p'))) \exp(-\mathcal{B}(t, p')\Delta t) \quad (20)$$

$$p' = \frac{a(t + \Delta t)p}{a(t)}. \quad (21)$$

In a homogeneous cosmology, T^{00} in Local Lorantz coordinate is the same as comoving coordinate and $T_{comov}^{ii} = a^2 T_{Loc.Lor.}^{ii}$.

4 Numerical Simulation

What makes numerical calculation of (18) to (20) difficult is the extension on roughly 34 orders of magnitude of energy from $10^{-9} eV$ (radio background) to $10^{24} eV$ (mass of UHDM) (from now on we call this energy range \mathcal{R}_E). Physical processes in this vast energy range have varieties of behavior, resonances, etc. Moreover, species have distributions which are orders of magnitudes different from each others. In other term these equations are very stiff. Semi-analytic method explained above helps to increase the precision of numerical calculation. However, the 5-dimensional integration in (14) is extremely time and memory consuming and it is impossible to determine it with the same precision.

In the following we describe in detail the numerical calculation of (18) to (20), as well as cosmology, initial conditions and backgrounds which have been used.

4.1 Multiplicity and Cross-section

For processes simulated by PYTHIA, we need to calculate total and differential cross-sections (see (12) and (14)). The former is given by the program itself. To determine the latter, we divide \mathcal{R}_E to logarithmic bins (one per order of magnitude) and classify particles according to their momentum in them. The angular distribution of produced particles with respect to the axis of incoming particles in CM also is divided linearly to 90 bins. at a given s , the cross section in each bin $\Delta\sigma_{ij} = \sigma_{tot}N_{ij}/N$. N_{ij} is the number of particles of a given species in bin ij . N is the total number of simulated events.

The same procedure is used for determination of $\frac{dM}{dp}$, the differential multiplicity of a particle in the decay of WIMPZILLA. Here it is not necessary to consider the angular distribution because in the rest frame of WIMPZILLA (that we consider to be the same as the Local Lorantz frame, as mentioned before), the decay has a spherical symmetry.

Because PYTHIA can not cover the totality of the energy range, for high energy bins we use a linear extrapolation in $\log p$. The contribution of these energies i.e. $E_{CM} \gtrsim 10^6 GeV$ on the evolution of species is nevertheless small because density of concerning particles is very low.

As mentioned above, for most processes including $p - \gamma$, PYTHIA can not simulate the interaction with $E_{CM} < 4\text{GeV}$. $p - \gamma$ is the most important processes for the energy dissipation of protons specially in this uncovered energy range where interaction with CMB photon is concentrated. In these energies we use directly the total cross-section obtained from experience [65]. For differential cross-section, we extrapolate angular distribution from higher energies and normalize it to the exact total cross-section.

4.2 Evolution Equations

In (12) and (14), the integrals over angular degrees of freedom can be separated from energy integrals and they don't depend on any cosmological or DM parameter. It is therefore very convenient to calculate them separately.

We divide each 180° interval to 9 bins and use trapezoid method for integration. For the single integral in (12) a better resolution with 90 bins has been used. However, our tests show that even the moderate resolution of 9 bins gives, up to a few percents, the same results as the more precise integration. This is a reassuring results and means that the triple integrals in production term also must be enough correct even with a low resolution.

Calculation of production term for first-order interactions is more complicate. They are processes of type $2\text{part.} \rightarrow 2\text{part.}$. In the CM frame where all cross-sections are determined, analytically or numerically, the incoming and outgoing particles have the same momentum. This is equivalent to having a Delta function in the integral. The numerical realization of this function specially with a moderate resolution of integration is very difficult. Consequently, one has to analytically absorb this function into integrand. Details of the calculation can be found in Appendix 2.

Numerical solution of evolution equation itself needs much better energy resolution due to stiffness of distributions. The resolution must be at least of the order of magnitude of smallest quantities. Our tests show that a division to 680 logarithmic bins of the energy range \mathcal{R}_E (i.e 20 bins per one order of magnitude) gives an acceptable compromise between precision and calculation time.

In place of fixing initial and final evolution time, we use the redshift because it is the physical quantity which is directly measured. We divide the interval $z = [z_{dec} - 0.001]$ to 30 logarithmic bins and the last step is from $z = 0.001$ to $z = 0$.

The program is written in C++ language and is highly modular. It can be requested from author. To test the precision of our numerical calculation, we have run the program without interaction terms. The error on total T^{00} is 0.7% and on non-baryonic DM is practically zero. For other species it is 5.5% to 7.5%. Including interaction terms but not the decay of DM gives the same answer. This test is crucial for correct simulation of thermal equilibrium of the Universe.

4.3 Cosmology Model and Initial Conditions

We consider a flat universe with present value of parameters as the followings: $\Omega_M = 0.3$, $\Omega_\Lambda = 0.7$, $h = H_0/100\text{km sec}^{-1}\text{Mpc}^{-1} = 0.7$ and $\Omega_b = 0.02h^{-2}$.

Evolution equations have been evolved from photon decoupling to today. We fix the decoupling redshift at $z_{dec} = 1100$. The distribution of species at that time was thermal with a temperature $T_{dec} = T_{CMB}(z_{dec} + 1) = 0.26\text{eV}$, $T_{CMB} = 2.728\text{K}$ [76] for e^\pm , p^\pm and γ and $\frac{4}{11}T_{dec}$ for ν and $\bar{\nu}$.

In the same way, one can determine the temperature of Dark Matter² at decoupling [77]:

$$T_{DM}(z_{dec}) = \frac{g_{*s}^{dec\frac{2}{3}} T_{dec}^2}{g_{*s}^{DM\frac{2}{3}} T_{DM}} \quad (22)$$

²One should consider T_{DM} more as an kinetic energy scale than a real temperature because if ultra heavy particles exist, they could never be thermalized.

T_{DM} is the decoupling temperature of the Dark Matter. If we assume that $T_{DM} \sim 10^{16} eV$, $T_{DM}(z_{dec}) < 10^{-18} eV$. Therefore, our approximation $T_{DM} = 0$ is quite justified.

We know the density of species at present. Their initial value at decoupling depends on the equation of state of the Universe. However, it is exactly what we want to calculate! Consequently, we have to determine their value at decoupling approximately by neglecting the effect of UHDM decay. As the lifetime of WIMPZILLA is assumed to be much longer than the age of the Universe, the present value of densities after evolution must stay very close to our initial assumption.

We *define* the initial densities as followings:

$$n_\gamma = n_{COBE}(z_{dec} + 1)^3 \quad n_\nu = n_{\bar{\nu}} = 3 \times \frac{4}{11} \times n_\gamma \quad (23)$$

$$n_p = \frac{\Omega_b \rho_c}{m_p} (z_{dec} + 1)^3 \quad n_{e^-} = n_p \quad n_{\bar{p}} = n_{e^+} = 0 \quad (24)$$

$$n_{DM} = \frac{\rho_c (\Omega_M - \Omega_{hot} - \Omega_b (1 + \frac{m_e}{m_p}))}{m_{DM}} (z_{dec} + 1)^3 \quad \Omega_{hot} = \frac{\pi^2}{30} g_* T_{CMB}^4. \quad (25)$$

Knowing initial density and temperature, other quantities like chemical potential and distributions can be determined [77]. We assume that the age of the Universe $\tau_0 = 14.8 Gyr$. This quantity also depends on the equation of state and we use it only for fixing the lifetime of WIMPZILLA.

4.4 Backgrounds

Apart from CMB and relic neutrinos which are included in the initial conditions, we don't include any other background to high redshift distributions. For $z \leq 3$, we add near IR to UV emissivity of stars [78] [79] to equation (20). Far IR which is very important for energy dissipation of UHECRs, is not added because there is very few information about its evolution with redshift. High energy backgrounds are not added because we want to be able to distinguish the contribution of remnants from other sources. Adding backgrounds by "hand" evidently violates the energy conservation of the model, but there is not any other simple alternative method. In addition, the violation is very small and comparable to numerical errors.

Here a comment is in order why we have included star backgrounds and not the synchrotron radiation. Star background is considered as an external source. By contrast, synchrotron radiation concerns high energy electrons which are involved in the evolution. In (1), the elimination of interaction with an external field in a homogeneous universe means that the probability for production and absorption of synchrotron photons is the same. It is not therefore possible to consider their production without their absorption i.e. interaction of electrons with external magnetic field.

5 Results

Figure 3 shows the energy flux of high energy protons and photons in a homogeneous universe. Fig.4 shows the same quantity for all species. The GZK cutoff is very transparent. With our background model it happens at $E \approx 10^{18.2} eV$. The steepness of the cutoff is understandable from very abrupt form of $p - \gamma$ cross-section at low energies [65]. However, we can not rule out the effect of moderate energy resolution of this simulation in the form and deepness of the trough.

According to this figure, even the shortest lifetime we have considered can not explain the observed flux of protons. On the same figure the flux without energy dissipation has been also shown. It is compatible with Ref. [59] which does not consider the energy dissipation of particles. In this latter case, the lifetime must be $\sim 4 - 6$ orders of magnitude larger than the age of the Universe. On the one hand, this results shows the rôle of a realistic model of energy dissipation in the estimation of mass and lifetime of UHDM. On the other hand, it proves the importance of clumping of Dark Matter, i.e. most of observed UHECRs

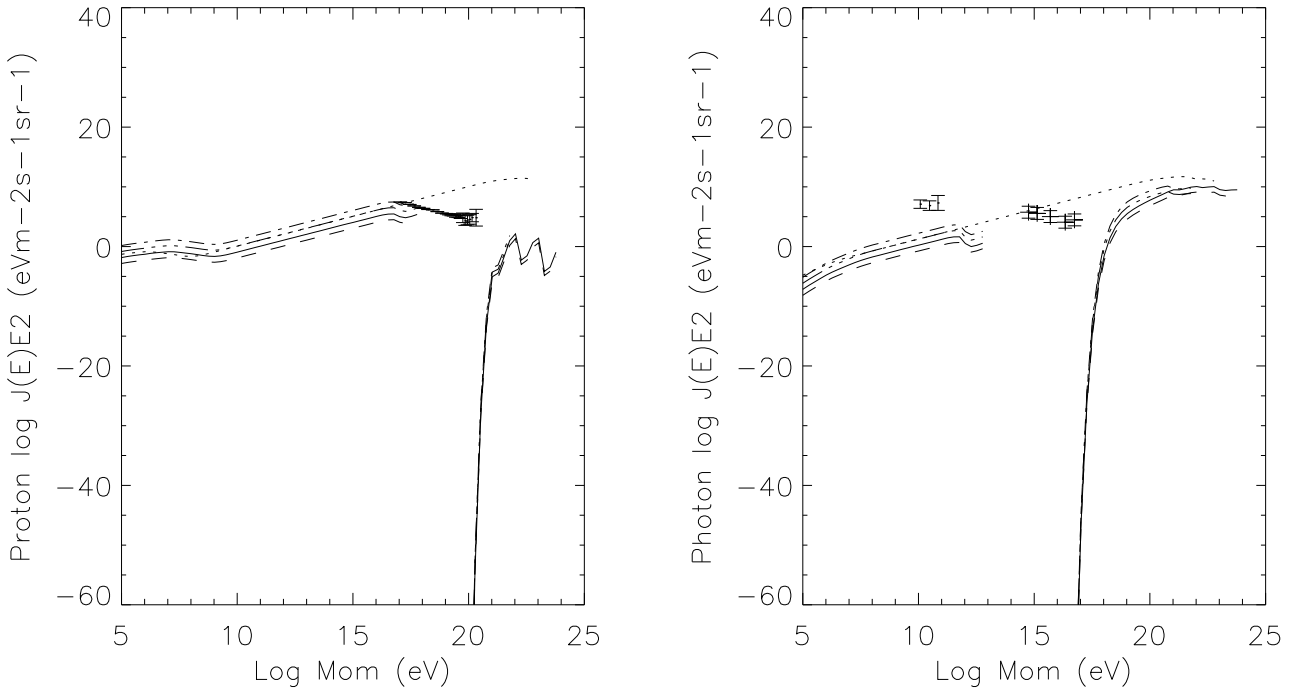


Figure 3: Energy flux for protons and photons. Solid line $m_{DM} = 10^{24}eV$, $\tau = 5\tau_0$, dashed line $m_{DM} = 10^{24}eV$, $\tau = 50\tau_0$, dash dot $m_{DM} = 10^{22}eV$, $\tau = 5\tau_0$, dash dot dot $m_{DM} = 10^{22}eV$, $\tau = 50\tau_0$. Dot line is the spectrum without energy dissipation. For protons data from Air Showers detectors [13] is shown. Data for photons are EGRET whole sky background [81] and upper limit from CASA-MIA [82].

must come from nearby sources. This conclusion is independent of the source of UHECRs.

In the case of decaying UHDM hypotheses, the most important source is the Galactic Halo. Before trying to make a simple model of halo in the next section, we discuss some of other conclusions that one can make from this study.

Fig.3 shows also the energy flux of photons. Taking into account the fact that $p - \gamma$ cross-section is $\sim 10^5$ times smaller than $p - p$, with present statistics of UHECRs, less than one photon shower could be observed.

The effect of clumpiness is less important for photons. In Fig.3 the data from EGRET for $10^8 eV < E < 10^{11} eV$ is compared with our calculation. Not only it is compatible with a lifetime of $\tau = 5\tau_0$, but also it shows a positive slope similar to the prediction of UHDM where the contribution of the decay of UHDM becomes important. Therefore, future observations of GLAST at $E > 10^{11} eV$ is crucial for understanding the source of UHECRs.

Fig.5 illustrates the total optical depth, i.e. $\mathcal{B}(t, p)$ in equation (12), of high energy particles and contribution of backgrounds at $z = 0$. It shows that for protons, even a source at $\sim 20 Mpc$ must be very strong to be able to provide the observed flux. The optical depth of protons is even larger than what we have obtained here because we didn't take into account the far IR background. This makes difficulties for the recent suggestion by Ahn E.J., *et al.* [40] that Virgo cluster can be the only source of UHECRs, even if the magnetic field of Galactic wind is as strong as what is considered in that work. The main challenge is finding a conventional source with enough emissivity of CRs at ultra high energies.

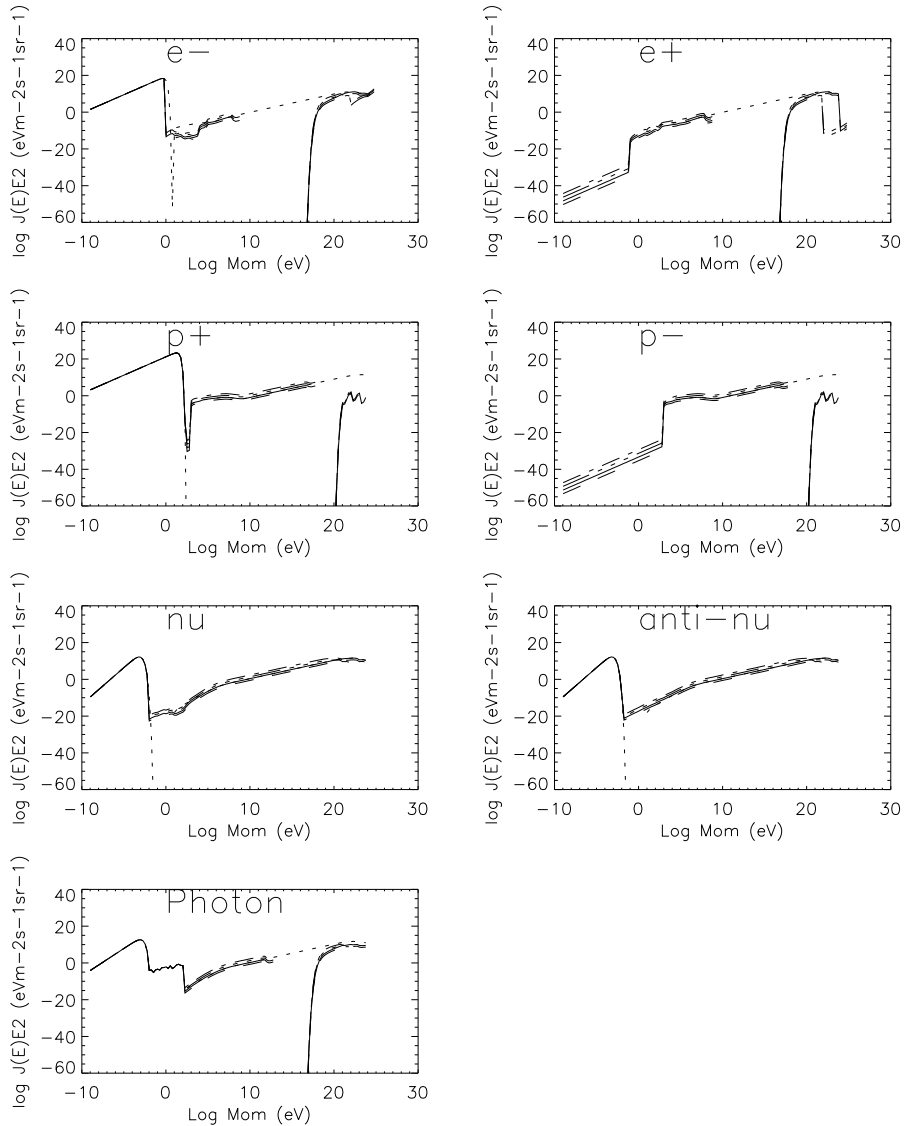


Figure 4: Energy flux of stable species. Description of curves is the same as Fig.3.

5.1 CMB Distortion and Entropy Excess

To see if a relatively short life UHDM can distort CMB, we reduced the flux spectrum from the spectrum with a stable DM. Fig.6 shows the result for $z = 0$. Up to energies much higher than CMB, there is no distortion at least up to 1 to 10^8 parts. The distortion of CMB anisotropy will be studied elsewhere. We have also examined the entropy excess separately for each species. There is no entropy enhancement except for e^+ and p^- which in our model are absent from the initial conditions. Comparing to other species, their contribution is very small and negligible.

5.2 Baryon and Lepton Asymmetry Generation

It has been suggested [80] [22] that the decay of UHDM may be able to generate additional baryon and lepton asymmetry. At GUT scale, i.e. the mass scale of WIMPZILLA, we expect such processes and the fact that a late time decay is out of thermal equilibrium and satisfies Sakharov conditions for baryogenesis [77] make growing asymmetry plausible.

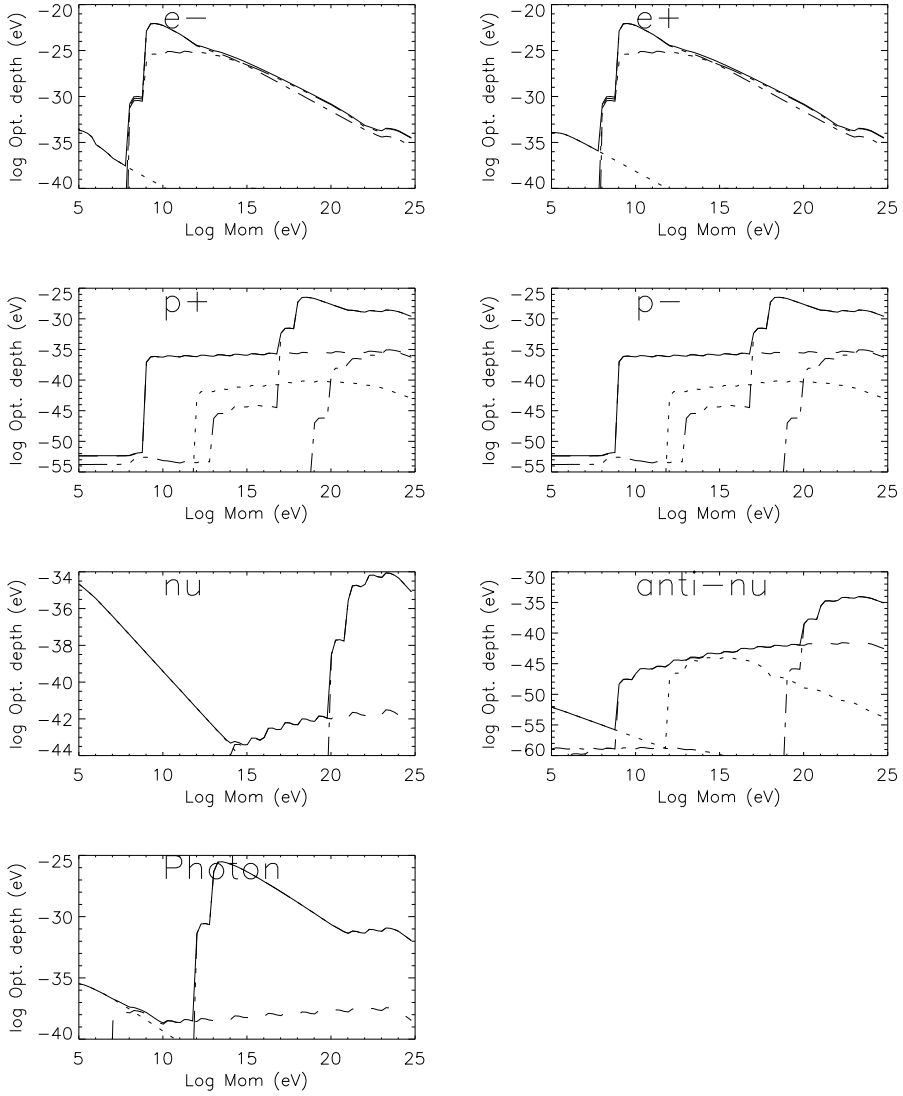


Figure 5: Total optical depth of species and contribution of backgrounds. Solid line is total optical depth, dot line contribution of e^\pm , dashed line p^\pm , dash dot $\nu & \bar{\nu}$, and dash dot dot dot γ . Dependence on lifetime and mass of UHDM is negligible.

The rate of baryonic/leptonic number production by decay of UHDM in comoving frame can be expressed as:

$$\frac{d(n_b - n_{\bar{b}})}{dt} + 3 \frac{\dot{a}(t)}{a(t)} (n_b - n_{\bar{b}}) = \frac{\varepsilon n_{DM}}{\tau}. \quad (26)$$

ε is the total baryon number violation per decay. The solution of this equation is:

$$\Delta(n_b - n_{\bar{b}}) = \varepsilon n_{DM}(t_0) (1 - \exp(-\frac{t - t_0}{\tau})) \frac{(1 + z_0)^3}{(1 + z)^3}. \quad (27)$$

$$\Delta B \equiv \frac{\Delta(n_b - n_{\bar{b}})}{2g_* n_\gamma} = \frac{\varepsilon n_{DM}(t_0)}{2g_* n_\gamma(t_0)} (1 - \exp(-\frac{t - t_0}{\tau})) \frac{(1 + z)}{(1 + z_0)}. \quad (28)$$

If $t_0 = t_{dec}$, $\frac{n_{DM}(t_0)}{n_\gamma(t_0)} \sim 10^{-22}$ (for $m_{DM} = 10^{24} eV$). Therefore $\Delta B \sim 10^{-22} \varepsilon$ at $z = 0$. As ε can not be larger than total multiplicity, ~ 1000 , $\Delta B \lesssim 10^{-16}$, i.e. much smaller than primordial value $\sim 10^{-10}$.

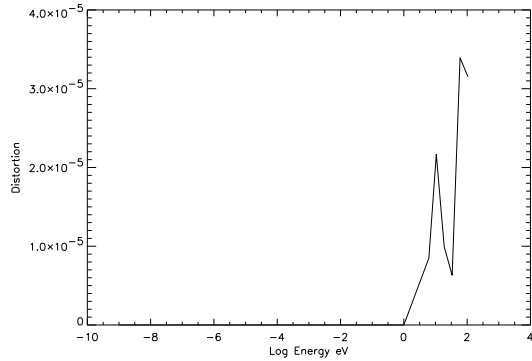


Figure 6: Fraction of distortion in photon distribution with respect to a stable DM.

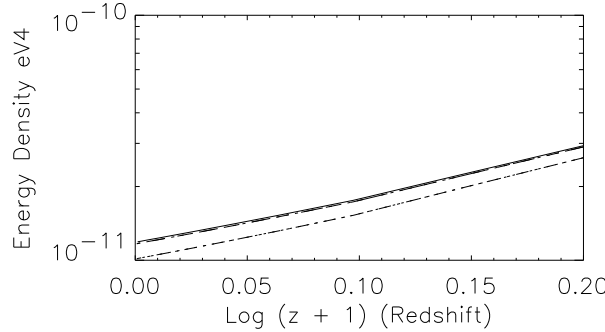


Figure 7: Energy density of the Universe. Solid line a stable DM, dash line $\tau = 50\tau_0$, dash dot $\tau = 5\tau_0$. Dependence on the mass of UHDM is negligible.

We tested this argument by assuming $\varepsilon = 0.1$ at all energies, i.e. $\varepsilon_{tot} = 0.1\mathcal{M}_{tot}$. Evidently $n_{\bar{p}}$ is smaller, but the change of n_p is too small to be measured. The same is true for number density of leptons, but there is a small increase in energy density of leptons with respect to anti-leptons comparable to ε .

5.3 Equation of State of the Universe

Decay of UHDM gradually changes part of CDM to HDM and thus changes the equation of state of the Universe. Fig.7 shows the variation of equation of state. For $\tau \sim 50\tau_0$ or larger, it would be too small to be measurable. For smaller τ , DM decay plays the rôle of a running cosmological constant. A complete study of this issue and comparison with data is under preparation.

6 Halo

To see the effect of clumping of a decaying UHDM on the flux of UHECRs, here we try to make a very simple model. A complete treatment of halos will be reported elsewhere.

We consider a halo as a uniform over-density at $z = 0$. By putting $a(t) = cte$, it is possible to use the model developed for homogeneous universe to study the propagation of decay remnants.

Energy binning for cross-sections and evolution equation is taken to be the same as homogeneous universe case. Because we want to study the propagation of remnants in a volume comparable to the Galactic

Halo, we consider time steps equivalent to 10kpc . Our tests show that after a few steps (~ 7), the accumulation rate of ultra high energy particles becomes very slow. We consider two cases. In the first case we simply evolve distributions for a number of steps (up to 30). In the second case, after some steps, we stop the decay of the Dark Matter to simulate a halo of MACHOs, presumably baryonic matter [83]. Then, the evolution is continued for more 5 steps to simulate propagation through MACHO halo.

Evidently this model is very approximative. We use it only to make a crude estimate of production and absorption of UHECRs.

6.1 Initial Conditions and Galactic Backgrounds

Galactic baryonic matter is taken to have a thermal distribution with $T_b = 10^4\text{K}$. We assume that baryonic over-density is biased with respect to DM i.e. the fraction of baryons to DM is larger than its mean value in the Universe. With these assumptions the initial number densities can be expressed as:

$$\begin{aligned} n_p &= \frac{b\delta\rho_c}{m_p} & n_{e^-} &= n_p \\ n_{\bar{p}} &= n_{e^+} = 0 \\ n_{DM} &= \frac{(1-b)\delta\rho_c}{m_{DM}} \end{aligned} \quad (29)$$

b is the fraction of baryons in the halo. In the following $b = 0.3$, i.e. ~ 2 times primordial value [84] in the cosmological model explained above. δ is the mean over-density of the Halo. Inspired by universal halo density distribution of NFW [85], we consider a halo with characteristic radius (i.e. virial radius) $r_{200} = 0.1\text{Mpc}$. According to NFW distribution and by definition this means $\delta = 200$. These parameters defines a halo of mass $M_H = 6 \times 10^{12} M_\odot$.

Neutrino density is assumed to be the same as relic at $z = 0$. For photons, in addition to CMB, we consider a galactic background as the following:

Galactic IR and visible backgrounds are not very well known. We use the results of the model developed by DIRBE group for detection of extragalactic component of the IRB [86]. We consider the observed value of IRB after elimination of Inter-Planetary Dust (IDP) contribution as the galactic background. It is just an estimation of average galactic IRB. It is not clear if we can extend the local value of IRB to whole galaxy or take it as a representative average. For this reason we also increase it 10 times (probably an extremely high value) to see the effect in the energy dissipation of UHECRs (see below for conclusions). Our simulation does not include radio background.

For soft and hard X-Ray galactic backgrounds, we use the model developed for extraction of extragalactic component from ROSAT and ASCA observations [87]. It considers GXB as two thermal components, a soft component with $T_{sx} = 70\text{eV}$ from Local Bubble, and a hard component with $T_{hx} = 145\text{eV}$ from hot gas, probably in the Halo. We add also the extragalactic component for $0.25\text{keV} < E < 10\text{keV}$.

7 Results

Fig.8 shows the distribution of high energy protons and photons for a uniform halo and for a halo that its inner part is composed of MACHOs. Only the result for $m_{DM} = 10^{24}\text{eV}$ and $\tau = 5\tau_0$ is shown. The flux $E \sim 10^{20}\text{eV}$ is somehow higher than observation and the lifetime must be about one order of magnitude longer. A significant radio background however can extend the trough to higher energies and decrease the flux at $E \gtrsim 10^{20}\text{eV}$.

The trough of GZK cutoff is shallower than in the case of a homogeneous universe specially for a uniform halo without MACHOs. Because of importance of this part of the spectrum in the interpretation of results, Table 4 summarizes the numerical value of simulated and observed spectrum. The absence of real trough in the observations shows the importance of very nearby, i.e. galactic disk sources. The contribution of

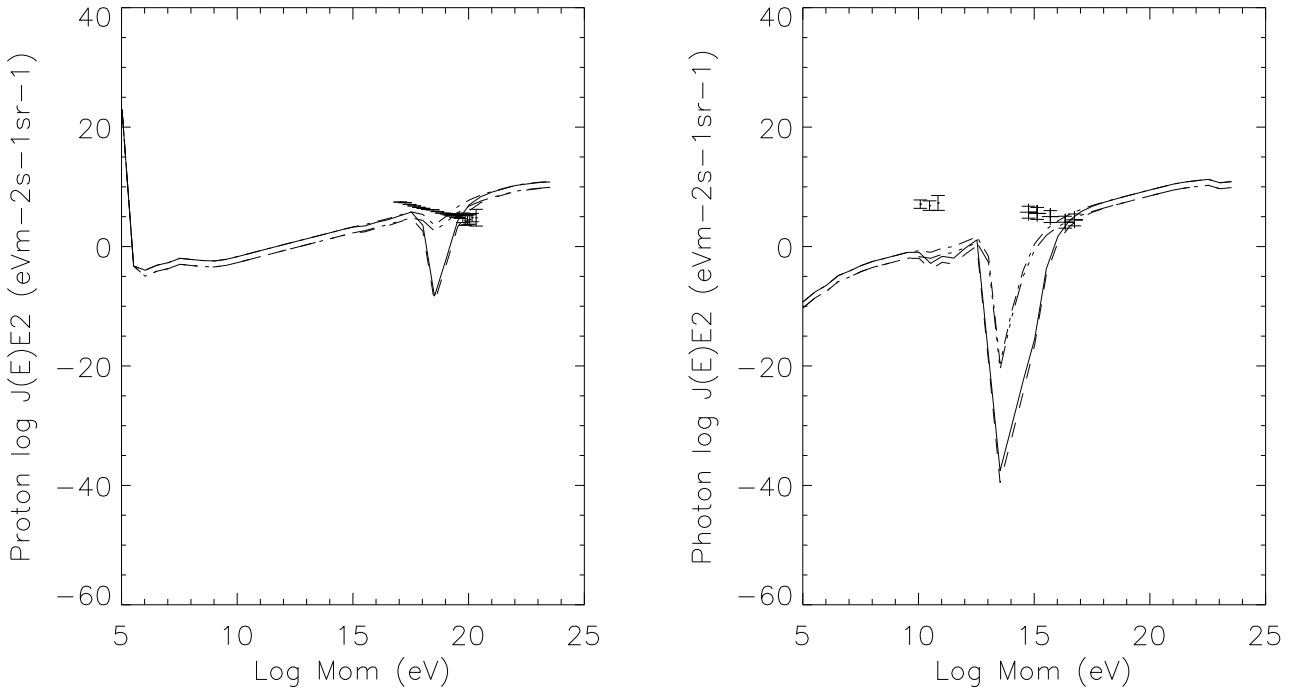


Figure 8: Flux of high energy protons and photons in a uniform clump. $m_{DM} = 10^{24} eV$, $\tau = 5\tau_0$ and $\tau = 5\tau_0$. Dash dot and dash dot dot dot lines presents UHDM halo. Solid and dashed lines show a halo of UHDM and MACHOs. Data is the same as in Fig.3.

local sources is also in agreement with AGASA observation of UHECR excess in the direction of galactic center at $E \sim 10^{18} eV$. At these energies conventional sources must yet have a significant contribution. However, as the cutoff finishes after $E \gtrsim 10^{19} - 10^{20} eV$, even if the spectrum of these sources can be extrapolated with the same slope to higher energies, it can not explain the rising slope of UHECRs. As the IR background is crucial for energy dissipation of UHECRs, we increased it to 10 times of DIRBE model to see the effect. Proton flux at high energies decreases $\sim 3 - 4$ times. This amount of IR background is probably too high. But this test shows the importance of observation/modeling of Galactic backgrounds for understanding the origin of UHECRs and characteristics of a hypothetic UHDM.

We don't want to make any strong conclusion from this very crude model of halo, but it seems that a decaying UHDM with $\tau \sim 10 - 100\tau_0$ is compatible with present observations.

We have also tested the distortion of CMB by remnants as described for a homogeneous universe. There is no distortion up to at least 1 to 10^8 parts.

8 Conclusions

The main purpose of this work was showing the importance of a realistic cosmological model for finding the answer to the mystery of UHECRs and introducing readers to the program that has been developed for achieving this goal.

We showed that the lifetime of UHDM can be $\sim 10 - 100\tau_0$ much shorter than what has been suggested in some previous works. Therefore the cosmological implication of a UHDM can be more important.

We have studied a special decay mode. Any other mode that produces *invisible* WIMPs or leptonic or semi-leptonic modes decreases the lifetime of UHDM. If more nucleon are produced the lifetime must be

longer but it seems less probable than other cases.

Some of our conclusions like the predominance of nearby sources, specially the halo of our galaxy is independent of the source of UHECRs and limits possible conventional candidates.

We showed the reciprocal influence of UHECRs and backgrounds on each others. Consequently, whatever the source of UHECRs, it is extremely important to correlate their observations to observation of high energy photon and neutrino backgrounds.

This work is the first step to a comprehensive study of effects of a decaying Dark Matter. Other issues like a realistic model for halos, effects on the determination of cosmological parameters and equation of state and comparison with more data from cosmic rays and high energy backgrounds remain for future works.

Appendix 1: Fragmentation in MLLA

The MLLA treats fragmentation as a Markov-chain. Consequently, the differential multiplicity is proportional to splitting function $P(x)$ (See e.g. [68]):

$$\frac{d\mathcal{M}(x_E)}{dx_E} \propto P(x) \quad x_E = \frac{E}{E_j}. \quad (30)$$

For a gluon jet and at $x_E \ll 1$, $P(x_E) \sim \frac{1}{x_E}$, and one expects that:

$$\frac{d\mathcal{M}(x_E)}{d(\ln(x_E))} \propto \text{Total Num. of splitting} \propto E_j. \quad (31)$$

Apparently at high energies $E \gtrsim 100\text{GeV}$, increasing CM energy just increases the probability of having more high energy fragments which simply escape fragmentation. A consequence of this behavior is the narrowing of the multiplicity distribution (See Fig.9) in contrast to theoretical prediction i.e. KNO [88] scaling for $E_j \rightarrow \infty$. This limit is obtained at parton level. However, if LPHD is valid, one expects the same type of behavior at hadron level. Another factor that can explain, at least partially, the deviation from theory is the decay of hadrons in our simulation. It increases total multiplicity more than its statistical variation and makes the distribution narrower. But it can not explain the absence of large deviation from mean value. Even after decay these events should keep their difference with average. As both MLLA and Monte Carlos fail to reproduce observations in relatively low energies [66] [70], the exact behavior at high energies is not clear.

Appendix 2: Production Integral for $2 \rightarrow 2$ Processes

Cross-sections are Lorantz invariant. However, to have a unique expression for what are simulated and what are calculated analytically, we determine all of them in their CM.

The triple integral in (14) depends on three momentum variables corresponding to the momentum of two incoming particles and one of the outgoing particles that its evolution is under calculation. In the case of a $2 \rightarrow 2$ process, the amplitude of the momentum of final particles depends only on s .

$$p = (E_i, p_i \cos \phi_i \sin \theta_i, p_i \sin \phi_i \sin \theta_i, p_i \cos \theta_i). \quad (32)$$

is the 4-momentum of outgoing particle, and p'_i is its counterpart in the CM:

$$p'^2_i = \frac{(s - m_3^2 - m_4^2)^2 - 4m_3^2m_4^2}{4s}. \quad (33)$$

$$p'_i = \Gamma p_i \quad (34)$$

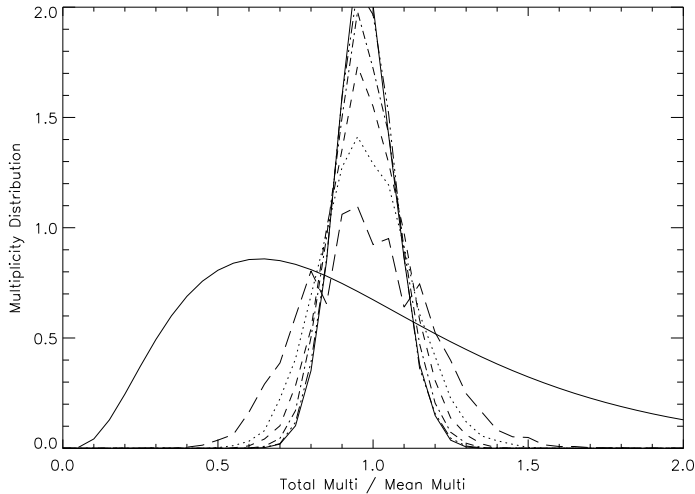


Figure 9: Distribution of multiplicity in hadronization of a pair of gluon jets. Solid line is the highest energy $E_{CM} = 10^{20} eV$; Long dash is lowest energy $E_{CM} = 10^{11} eV$. KNO distribution is shown also (solid line).

m_3 and m_4 are the mass of out-going particles, Γ is the boost matrix. The equality of two expressions for p'_i leads to an equation that can be solved for one of the angular variables in (32). The calculation is tedious but strait forward. With respect to ϕ_i , the equation is 4th order but in the case of a homogeneous cosmology where the boost matrix depends only on the relative angle between incoming particles, it depends only on $\tan^2(\frac{\phi_i}{2})$ and is analytically solvable. In this way the integration over ϕ_i in (14) reduces to sum of integrand evaluated at the roots of the equation.

This method provides a general way to deal with this problem and is easier than doing calculation for each cross-section separately.

Acknowledgement I would like to thanks people of Strasburg Observatory for their kindness.

References

- [1] Chung D., Kolb E. W., Riotto A., hep-ph/9810361.
- [2] Chung D., Kolb E. W., Riotto A., *Phys. Rev. D* **59**, 023501 (1999), Kuzmin V. & Tkachev I., *JETPhys. Lett.* **68**, 271 (1998), Chung D., hep-ph/9809489.
- [3] Ellis J., Lopez J.L., Nanopoulos D.V. *Phys. Lett.* B245375 1990.
- [4] Witten E., *Nucl. Phys. B* **471**, 135 (1996).
- [5] Benakli K. *et al.*, *Phys. Rev. D* **59**, 047301 (1999).
- [6] Giudice G.F. & Rattazzi R. hep-ph/9801271.
- [7] Hamaguchi K., Nomura Y., Yanagida T., *Phys. Rev. D* **58**, 103503 (1998), *Phys. Rev. D* **59**, 063507 (1999).
- [8] Kofman L., Linde A., Starobinsky A. A. *Phys. Rev. Lett.* **73**, 3195 (1994), *Phys. Rev. D* **56**, 3258 (1997), Khlebnikov, S. & Tkachev I., *Phys. Rev. Lett.* **77**, 219 (1996), *Phys. Rev. Lett.* **79**, 1607

(1997), Felder G., Kofman L., Linde A., *Phys. Rev. D* **59**, 123523 (1999), Giudice G.F. *et al.*, *J. High Ener. Phys.* **9908**, 014 (1999).

[9] Griest K., Kamionkowski *Phys. Rev. Lett.* **64**, 615 (1990).

[10] Egorov T. A., Proc. Tokyo Workshop on Techniques for the Study of Extremely High Energy Cosmic Rays (ICRR University of Tokyo) p35 (1993).

[11] Bird D.J. *et al.*, *ApJ.* **424**, 491 (1994).

[12] Hayashida N. *et al.*, *Phys. Rev. Lett.* **73**, 3491 (1994), Yoshida S. *et al.*, *Astropart. Phys.* **3**, 105 (1995).

[13] Yoshida Sh. & Dai H., *J. Phys. G: Nucl. Part. Phys.* **24**, 905 (1998).

[14] Greisen, K., *Phys. Rev. Lett.* **16**, 748 (1966), Zatsepin G.T. & Kuzmin V.A., *JETPhys. Lett.* **4**, 78 (1966).

[15] Takeda M. *et al.*, astro-ph/9902239.

[16] Wiebel-Sooth & Biermann, Landolt-Börnstein vol. VI/3c, Springer Verlag, 37, (1999).

[17] Halzen F. *et al.*, *Astropart. Phys.* **3**, 151 (1995), Boothby K. *et al.*, *ApJ.* **491**, L35 (1997). Cillis & Sciutto astro-ph/9908002.

[18] Abu-Zayyad, *et al.*, astro-ph/9911144.

[19] Anchordoqui L.A., *et al.*, *Phys. Rev. D* **59**, 094003 (1999),

[20] Stecker F.W. & Salamon M.H., *ApJ.* **512**, 20 (1999), Anchordoqui L.A., *et al.*, *Phys. Rev. D* **60**, 103001 (1999), astro-ph/9912081.

[21] Epele L.N. & Roulet E., *J. High Ener. Phys.* **10**, 009 (1998).

[22] Bhattacharjee P. & Sigl G., astro-ph/9811011.

[23] Blandford R. astro-ph/9906026.

[24] Wandel A., astro-ph/9709133.

[25] Yock, P., in "Black Holes & High Energy Astrophysics", Ed. Sato H. & Sugiyama N., Frontier Science Series No. 23, Universal Academy Press, Tokyo, (1998), Normille, D., *Science* **284**, 734 (1999), Abe F. *et al.*, astro-ph/9911398.

[26] Rachen J.P., Biermann P.L., *A&A* **272**, 161 (1993), Ostrowski astr-ph/9803299.

[27] Halzen F, Vazquez R., Stanev T. & Vankov H.P., *Astropart. Phys.* **3**, 151 (1995), Halzen F. astro-ph/9704020.

[28] Boldt E. & Ghosh P., astro-ph/9902342.

[29] Biermann P.L., astro-ph/9501006.

[30] Mannheim K., Protheroe R.J. & Rachen J.R., astro-ph/9812398.

[31] Miralda-Escudé J., Waxman E., *ApJ.* **462**, L59 (1996), Waxman E., astro-ph/9612061, Totani T., astro-ph/9810206, *Astropart. Phys.* **11**, 451 (1999).

[32] Waxman E., Coppi P., *ApJ.* **464**, L75 (1996).

- [33] Achterberg A. *et al.* astro-ph/9907060.
- [34] Harari D. *et al.*, JHE **08**, 022 (1999), Farrar G.R., Piran T., astro-ph/9906431.
- [35] Sigl G. *et al.*, *Astropart. Phys.* **10**, 141 (1999).
- [36] Blasi P., Olinto A.V., *Phys. Rev. D* **59**, 023001 (1999).
- [37] Medina Tanco G.A., de Gouveia Dal Pino E. & Horvath J.E., astro-ph/9901053.
- [38] Stanev T. *et al.*, *Phys. Rev. Lett.* **75**, 3056 (1995), Uchihori Y. *et al.*, astro-ph/9908139.
- [39] Elbert J.W., & Sommer P., *ApJ.* **441**, 151 (1995), Bird *et al.*, astro-ph/9806096, Hillas M. *Nature* **395**, 15 (1998), Takeda M. *et al.*, *Phys. Rev. Lett.* **81**, 1163 (1998).
- [40] Ahn E.J., *et al.*, astro-ph/9911123.
- [41] Malkov M.A., *ApJ.* **511**, L53 (1999).
- [42] Farrar G.R. & Biermann P.L., *Phys. Rev. Lett.* **81**, 3579 (1998), Chadwick *et al.*, astro-ph/9903346.
- [43] Fargion D., Mele B., astro-ph/9710029, astro-ph/9902024, Weiler T.J., *Astropart. Phys.* **11**, 303 (1999).
- [44] Waxman E., astro-ph/9804023, Blanco-Pillado J.J., Vázquez R.A. & Zas E., astro-ph/9902266.
- [45] Dubovsky S.L. & Tinyakov P.G., *Pisma Zh. Eksp. Teor. Fiz.* **68**, 99 (1998), *JETPhys. Lett.* **68**, 107 (1998),
- [46] Berezinsky V. & Mikhailov A.A., *Phys. Lett. B* **449**, 237 (1999)
- [47] Hayashida N. *et al.*, *Astropart. Phys.* **10**, 303 (1999), astro-ph/9906056.
- [48] Benson A., Smialkowski A. & Wolfendale A.W. *Astropart. Phys.* **10**, 313 (1999).
- [49] Medina Tanco G.A. & Watson A.A., *Astropart. Phys.* **12**, 25 (1999).
- [50] Bhattacharjee P., Hill C.T., Schramm D.N., *Phys. Rev. Lett.* **69**, 567 (1992).
- [51] C.T. Hill, *Nucl. Phys. B* **224**, 469 (1983), C.T. Hill, D.N. Schramm & T.P. Walker, *Phys. Rev. D* **36**, 1007 (1987), Sigl G, Lee S., Schramm D.N., Bhattacharjee P., 1994 (3), Sigl G, Bhattacharjee P., Schramm D.N., astro-ph/9403093, Sigl G., *Space Sci. Rev.* **75**, 375 (1996), Bhattacharjee P., *Phys. Rev. Lett.* **81**, 260 (1998).
- [52] Vilenkin A., Shellard E.P.S., "Cosmic Strings and Other Topological Defects", Cambridge University Press, Cambridge (1994).
- [53] Albrecht A., Battye R.A., Robinson J., *Phys. Rev. Lett.* **79**, 4736 (1997), Turok N., Pen U.L., Seljak U., *Phys. Rev. D* **58**, 506 (1998), Pen U.L., Seljak U., Turok N., *Phys. Rev. Lett.* **79**, 1611 (1997), Albrecht A., Proceedings of the "International Workshop on Particle Physics and the Early Universe" Ambleside, September 1997, L. Roszkowski Ed.
- [54] Contaldi C., Hindmarsh M. & Magueijo J., *Phys. Rev. Lett.* **82**, 679 (1999), *Phys. Rev. Lett.* **82**, 2034 (1999).
- [55] Jedamzik K. Niemeyer J.C., *Phys. Rev. Lett.* **80**, 5481 (1998), *Phys. Rev. D* **59**, 124013 (1999), astro-ph/9901293.
- [56] Green A.M., *Phys. Rev. D* **60**, 063516 (1999).

[57] Bhattacharjee P., *Phys. Rev. D* **40**, 3968 (1989), Bhattacharjee P., Hill C.T., Schramm D.N., *Phys. Rev. Lett.* **69**, 567 (1992), Aharonian F.A., Bhattacharjee P., Schramm D.N., *Phys. Rev. D* **46**, 4188 (1992), Protheroe R.J. & Stanev T., *Phys. Rev. Lett.* **77**, (1996), Sigl G., Lee S. & Coppi P., astro-ph/9604093, Berezhinsky V. & Vilenkin A., *Phys. Rev. Lett.* **79**, 5202 (1997), Berezhinsky V., Kachelrieß & Vilenkin A., *Phys. Rev. Lett.* **79**, 4302 (1997), Bhattacharjee P., astro-ph/9803029, Berezhinsky V., Blasi P. & Vilenkin A., astro-ph/9803271.

[58] Lee S., *Phys. Rev. D* **58**, 043004 (1998).

[59] Birkel M. & Sarkar S., *Astropart. Phys.* **9**, 297 (1998).

[60] Ziaeepour H., Proc. of 2nd Intern. Workshop on the Identification of Dark Matter, Ed. Spooner N. & Kudryavtsev V., p. 106, World Scientific, 1999 (astro-ph/9811312).

[61] Kalashev O.E., Kuzmin V.A. & Semikoz D.V. astro-ph/9911035.

[62] Sjöstrand T., *Comp. Phys. Com.* 82741994. *Astropart. Phys.* **6**, 337 (1997), astro-ph/9707041, Medina Tanco G.A. astro-ph/9809219.

[63] Han T., Yanagida T. & Zhang R.J., *Phys. Rev. D* **58**, 095011 (1998), Farnk M, Hamidian H, & Puolamäki, *Phys. Rev. D* **60**, 095011 (1999).

[64] Felder G, Kofman L & Linde A., *Phys. Rev. D* **59**, 123523 (1999).

[65] Particle Data Group, *Review of Particle Physics*, *Europ. J. Phys. C* **3**, 227 (1998).

[66] DELPHI Collab. EPS-HEP99 paper 3-146, OPAL Collab. EPS-HEP99 paper 1-4, Abbiendi G. *et al.*, *Europ. J. Phys. C* **11**, 217 (1999).

[67] Muller A.H., *Phys. Rev. D* **4**, 150 (1971).

[68] Khoze V. A. & Ochs W., *Mod. Phys. A* **12**, 2949 (1997).

[69] Andersson *et al.*, *Phys. Rep.* **97**, 31 (1983), Sjöstrand, *Nucl. Phys. B* **248**, 469 (1984), *Int. J. Mod. Phys. A* **3**, 751 (1988).

[70] Webber B.R., hep-ph/9912292 and references therein.

[71] Landau L.D., Lifshitz E.M. & Berestetskii B., *Relativistic Quantum Theory*, Pergamon Press (1971).

[72] Hannestad S. & Madsen J., *Phys. Rev. D* **52**, 1764 (1995), Dolgov A.D., Hansen S.H. & Semikoz D.V., *Nucl. Phys. B* **503**, 426 (1997).

[73] Ehlers J., 1971, in "General Relativity and Cosmology", ed. B.K. Sachs, Academic Press New York.

[74] Tauber G.E. & Weinberg J.W., *Phys. Rev.* **122**, 1342 (1961), Weinberg S., *The Quantum Theory of Fields* Vol. I, Cambridge University Press, 1996.

[75] See for example Courant R. & Hilbert B. *Methods of Mathematical Physics*, John Wiley & Sons Inc. 1962.

[76] Mather J.C., *et al.* *ApJ.* **354**, L37 (1990).

[77] Kolb E. & Turner M., "The Early Universe", Addison Wesley Publ. Comp. (1990).

[78] Salamon M.H. & Stecker F.W., astro-ph/9704166.

[79] Valls-Gabaud D. & Vernet J., to appear in the proceedings of "Chemical Evolution from Zero to High Redshift", ESO, Garching, Germany, Oct. 1998.

[80] Ziaeepour H., in Proceedings of "From Quantum Fluctuations to Cosmological Structures", Casablanca 1-10 Dec. 1996, Ed. Valls-Gabaud D. *et al.*, ASPC Series vol. 126, p575, Ziaeepour H., in Proceeding of the "Large-Scale Structures: Tracks and Traces", Workshop, Potsdam, 15-20 Sep. (1997), Eds. Müller *et al.*, World Scientific 1998, p. 57.

[81] Sreekumar P., *et al.*, astro-ph/9709257.

[82] Chantell M.C., *et al.*, *Phys. Rev. Lett.* **79**, 1805 (1997).

[83] Alcock C., *et al.*, *ApJ.* **486**, 697 (1997), Fields B., Freese K. & Graff D.A., astro-ph/9804232.

[84] Jenkins A., *et al.*, *ApJ.* **499**, 21 (1998).

[85] Navarro J., Frenk C. & White S., astro-ph/9611107.

[86] Arendt R.G., *et al.*, *ApJ.* **508**, 74 (1998).

[87] Miyaji T., *et al.*, astro-ph/9803320.

[88] Polyakov A.M. *Sov. Phys. JETP* **32**, 296 (1971), *Sov. Phys. JETP* **33**, 850 (1971), Koba Z., Nielsen H.B., & Olesen P., *Nucl. Phys. B* **40**, 317 (1972).

Table 3: Interactions

Interaction	Analyt. Cal. E_{CM} Rang	Cuts	PYTHIA E_{CM} Rang	PYTHIA Parameters	Ref. Analytic Cross-Sec.
$e^\pm - e^\pm$ elastic	All	$\frac{s-4m_e^2}{m_e^2} > 10^{-3}$, $ \frac{t}{s} > 10^{-2}, \frac{u}{s} > 10^{-2}$	-	-	[71]
$e^+ - e^-$ elastic	$E_{CM} \leq 4GeV$	"	included in $e^+ - e^-$ $\rightarrow \dots$	- -	" "
$e^+ - e^- \rightarrow 2\gamma$	"	"	"	-	"
$e^+ - e^- \rightarrow \dots$	-	-	$4GeV \leq E_{CM} \leq 10^6$	Init. Braamst.	-
$p^\pm - e^\pm \rightarrow \dots$ (all combinations)	-	-	"	-	-
$p^\pm - p^\pm \rightarrow \dots$ (all combinations)	-	-	$3GeV \leq E_{CM} \leq 10^5$	-	-
$\nu - e^-$ elastic	All	$\frac{s-m_e^2}{m_e^2} > 10^{-3}$	-	-	[72]
$\bar{\nu} - e^+$ elastic	"	"	-	-	"
$\nu - e^+ \rightarrow \dots$	-	-	$4GeV \leq E_{CM} \leq 10^6$	-	-
$\bar{\nu} - e^- \rightarrow \dots$	-	-	"	-	-
$\nu - p^\pm \rightarrow \dots$	-	-	$4GeV \leq E_{CM} \leq 10^6$	-	-
$\bar{\nu} - p^\pm \rightarrow \dots$	-	-	"	-	-
$\nu - \bar{\nu}$	-	-	"	-	-
$\gamma - e^\pm \rightarrow \gamma - e^\pm$	$E_{CM} \leq 4GeV$	$\frac{s-m_e^2}{m_e^2} > 10^{-3}$, $ \frac{t}{s} > 10^{-2}, \frac{u}{s} > 10^{-2}$	-	-	[71]
$\gamma - e^\pm \rightarrow \dots$	-	-	$4GeV \leq E_{CM} \leq 10^6$	-	-
$\gamma - p^\pm \rightarrow \dots$	$1GeV < E < 4GeV$	-	"	$E_{CM}^{min} = 1GeV$, $p_t^{min} = 0.5GeV$, Singul. Cut = $0.25GeV$	[65]
$\gamma - \gamma \rightarrow e^+ - e^-$	$E_{CM} \leq 3GeV$	$\frac{s-m_e^2}{m_e^2} > 10^{-3}$, $ \frac{t}{s} > 10^{-2}, \frac{u}{s} > 10^{-2}$	-	-	[71]
$\gamma - \gamma \rightarrow \dots$	-	-	$3GeV \leq E_{CM} \leq 10^6$	-	-

Table 4: Energy flux of UHECRs close to GZK cutoff.

$\log(E)eV$	MACHO Halo $\log E^2 J(E)$ $m^{-2} \text{ sec}^{-1} \text{ sr}^{-1}$	Unif. Halo $\log E^2 J(E)$ $m^{-2} \text{ sec}^{-1} \text{ sr}^{-1}$	Observed $\log E^2 J(E)$ $m^{-2} \text{ sec}^{-1} \text{ sr}^{-1}$
17.025	3.76	3.86	7.45
17.525	4.38	4.41	7.
18.025	2.17	3.97	6.45
18.525	-9.70	2.20	6.1
19.025	-3.53	3.66	5.5
19.525	2.88	5.27	5.05
20.025	5.60	6.40	5.5
20.525	6.96	7.22	~ 5
21.025	7.74	7.83	